Journal of Hydrology 617 (2023) 128801

Contents lists available at ScienceDirect

Journal of Hydrology

journal homepage: www.elsevier.com/locate/jhydrol

Soil frost controls streamflow generation processes in headwater catchments

Mariel W. Jones [a,b,*], Stephen D. Sebestyen [c], Salli F. Dymond [d], G.H. Crystal Ng [b,e], Xue Feng [a,b]

[a] Department of Civil, Environmental, and Geo- Engineering, University of Minnesota, Twin Cities, Minneapolis, MN, USA
[b] Saint Anthony Falls Laboratory, University of Minnesota, Twin Cities, Minneapolis, MN, USA
[c] Northern Research Station, USDA Forest Service, Grand Rapids, MN, USA
[d] School of Forestry, Northern Arizona University, Flagstaff, AZ, USA
[e] Department of Earth and Environmental Sciences, University of Minnesota, Twin Cities, Minneapolis, MN, USA

ARTICLE INFO

This manuscript was handled by N Basu, Editor-in-Chief, with the assistance of Genevieve Ali, Associate Editor.

Keywords:
Peatlands
Streamflow generation
Long-term data
Snow

ABSTRACT

The relationship between snowmelt and spring streamflow is changing under warming temperatures and diminishing snowpack. At the same time, the hydrologic connectivity across catchment landscape elements, such as snowpack and surface wetlands, can play a critical role in controlling the routing of snowmelt to streams. The role of hydrologic connectivity is important in headwater regions of the continental northern latitudes, where catchments have low topographic relief and seasonally frozen ground. Nevertheless, the effects of soil frost on the sequence, timing, and magnitudes of hydrologic events that drive the movement of water from a snowpack to a stream are not fully understood. Therefore, we examine two questions: First, what is the flowpath that snow melt and precipitation from spring rain events takes to generate spring streamflow, and second, what hydrologic, climatic, or landscape variables exert the most control on the magnitude of streamflow? Here, we use long-term hydrological records from the two reference basins at the Marcell Experimental Forest in northern Minnesota to analyze the cascading effects across precipitation, snow, water table elevation, soil frost, and streamflow in peatland-dominated headwater catchments. We identify a sequence of fill-and-spill effects across the landscape that control the timing of spring streamflow generation. Then, we use stepwise regression to show that soil frost is a key supporting predictor for both the magnitude of streamflow in the spring as it adds significantly to the predictive power of precipitation and water table elevation. Our results highlight the importance of recognizing the role of soil frost, when present, on the partitioning of snowmelt between overland runoff and water table recharge during the critical snowmelt period, as well as the later partitioning between evapotranspiration and subsurface flows.

1. Introduction

In snow-dominated, seasonally-frozen catchments, spring streamflow timing and magnitude have been affected by a warming winter climate. For instance, estimates have shown that, over the last century, spring streamflow peaks have shifted earlier by 4.5 to 8.6 days in the northern hemisphere (Hodgkins and Dudley, 2006) and 8.7 to 14.3 days in the north-central United States (Ryberg et al., 2016). These shifts in streamflow responses partially result from decreases in snow pack size (Ford et al., 2020), including shifts in precipitation from snow to rain. Decreasing snowfall fraction, or the portion of precipitation falling in the form of snow, within a single catchment has been shown to lead to earlier spring streamflow peaks (Barnett et al., 2005), as well as decreases in mean annual streamflow (Berghuijs et al., 2014; Foster et al., 2016).

However, the influence of snow fraction on streamflow can be complicated by the direct effects of warming air temperature on the rate of snowmelt. Faster snowmelt rates, which can occur when spring warming arrives earlier, have been shown to lead to larger spring streamflow peaks and increased runoff and flood risk (Trujillo and Molotch, 2014). At the same time, warming temperatures can also increase surface energy and evapotranspiration later in the spring, which can have a counteracting effect that decreases streamflow (Badger et al., 2021). Even so, the relative importance of snow fraction versus temperature-driven land surface evaporative loss on streamflow remains unclear, with studies showing that either could serve as a dominant driver of streamflow in different future climate scenarios (Foster et al., 2016). Therefore, the complex interactions among climate, snow, and hydrological processes as the spring progresses remains an open research question.

The climatic effects on streamflow are mediated by the hydrologic connectivity on the landscape, which is controlled by a range of

* Corresponding author.
E-mail addresses: jone3247@umn.edu (M.W. Jones), feng@umn.edu (X. Feng).

https://doi.org/10.1016/j.jhydrol.2022.128801

Available online 7 December 2022

surface and subsurface storage components that accelerate or inhibit the flow pathways connecting water as precipitation inputs to streamflow (Pringle, 2003). For instance, snow–water equivalent (SWE), the total amount of water stored in a snowpack, represents a temporary storage of precipitation in a frozen state on the land surface, until it is released during the spring as snowmelt. This storage behavior temporarily "halts" the flow of water until it becomes available in liquid form again Musselman et al. (2021). As such, the timing of snow disappearance and the duration of snowmelt period exhibit strong influence on snowmelt runoff, streamflow peaks, and overall water availability in the spring. The relationships between snowmelt and streamflow are commonly studied in sites monitored using the SNOTEL network in the western United States (Leuthold et al., 2021; Heldmyer et al., 2021; Trujillo and Molotch, 2014), where, due to the well-defined surface topography and bedrock geology in mountainous regions, the flow path from snowmelt to streamflow is fairly direct (Schneider and Molotch, 2016). Surface wetlands represents another storage for precipitation. Surface wetlands may occur in areas of low topographic relief, and water within wetlands is stored until the water table elevation (WTE) increases over a threshold elevation, causing overland flow or lateral flow out of the wetland. The WTE to streamflow relationship is often the focus in studies on geographically isolated wetlands, which demonstrate clear connectivity among precipitation, WTE, and surface runoff (Cohen et al., 2016; Golden et al., 2016; Verry et al., 2011). In geographically isolated wetlands, the WTE is the most important predictor of landscape connectivity because it determines the level of isolation between the wetland and its surrounding surface water bodies (Winter and LaBaugh, 2003). As the height of the water table rises above the wetland surface levels, the excess water flows over the landscape to a surrounding stream, demonstrating the 'fill-and-spill' flow dynamics characteristic of hydrologic storage mechanisms (Cohen et al., 2016; Winter and LaBaugh, 2003; McDonnell et al., 2021; Leibowitz and Vining, 2003).

Despite the importance of snowpack and wetlands in determining the connectivity to and therefore timing and magnitude of streamflow, these near-surface storage components have rarely been studied together, especially in conjunction with another important landscape driver: soil frost. In areas of seasonally frozen ground, air temperature, snow, and soil moisture content control frost depths, which influence the snowmelt partitioning between overland flow and subsurface recharge (Aygün et al., 2019; Verry et al., 2011). Frozen ground restricts the infiltration of snowmelt and water table recharge, thereby increasing surface runoff (Zhao and Gray, 1999; Kane and Stein, 1983). The combined effects of rising winter temperatures and shrinking snowpack will also reduce the frost layer, resulting in an overall increase in the rate of groundwater recharge due to earlier snow melt and higher infiltration rates (Jyrkama and Sykes, 2007). The importance of frost is dependent on a diverse range of factors, some of which are difficult to predict or remain uncertain; while frost is more likely to affect streamflow in small catchments, cold climates and forested land cover can limit the effects frost has on streamflow (Ala-Aho et al., 2021). For example, a soil frost model developed using data from a catchment in northern Sweden showed no clear effect of soil frost on either the timing or magnitude of streamflow runoff. This lack of connection between frost and streamflow was likely due to limited frost occurrence (frost formed in only slightly more than half the years) or because the frost often had thawed before spring melt and streamflow onset (Lindström et al., 2002). In contrast, at a site in southern Switzerland, only 25%–35% of the melt water infiltrated into the soil in a winter with thin snowpack and thick frost layer, compared to 90%–100% in a different winter that had a deep snowpack and thin frost layer (Bayard et al., 2005).

As the effect of frost is variable across catchments and its presence can greatly affect spring runoff, it is important to consider that, first, soil frost can be quite heterogeneous across the landscape, a variability that is not captured in soil profile studies (Zhao and Gray, 1999; Kane and Stein, 1983). Second, soil frost varies from year to year, depending on winter climate and precipitation. Capturing these spatial and temporal variations is key to better understanding the relationship between soil frost and streamflow generation. In this study, we use long-term climatological and hydrological data to show a clear cascade of hydrological connectivity throughout the landscape and to determine the relative strengths of climatic and land surface variable in predicting annual streamflow trends.

Peatlands provide an ideal environment in which to study interacting surface and subsurface flows in the spring snowmelt season. The majority of peatlands are located in northern latitudes, where seasonal soil frost is becoming more dynamic under climate change, as soils transition from permanently frozen to seasonally frozen soils (Bridgham et al., 2013). Additionally, wetlands, including peatlands, are the single largest natural source of methane, contributing about a third of total global emissions (Gorham, 1991), with methane emissions from peatlands strongly controlled by seasonal water table dynamics and snowmelt dynamics (Feng et al., 2020). Therefore, it is critical to understand how the increasingly dynamic frost conditions will impact wetland water table, and by consequence, the role that peatlands play in both global and regional methane budgets. Regionally, headwater streams and wetlands provide innumerable ecosystem services, including regulating streamflow responses and improving downstream water quality (Colvin et al., 2019; Alexander et al., 2007). This critical hydrological landscape provides the ideal location to examine the effects of shifting spring hydrologic cascades on the wider network of low-relief catchments.

We focus on relationships among climate, hydrology, and landscape elements by examining two questions related to hydrologic connectivity in snow-dominated, low-relief peatland catchments: how do snow, frost, and surface wetlands mediate the flow paths from precipitation to spring streamflow? And what hydrologic, climatic, or landscape variables most control the magnitude of streamflow? As the effect of frost is variable across catchments and its presence can greatly affect spring runoff, it is important to consider that, first, soil frost can be quite heterogeneous across the landscape, a variability that is not captured in soil profile studies (Zhao and Gray, 1999; Kane and Stein, 1983). Second, soil frost varies from year to year, depending on winter climate and precipitation. In this study, we will examine these questions in two peatland catchments at the Marcell Experimental Forest (MEF) in northern Minnesota (USA), using statistical approaches applied to the analysis of long-term datasets. By focusing on two watersheds with long data records, we contribute new findings to both unresolved complexities of the importance of soil frost in forested catchments and expand upon existing soil profile, event-scale, and modeling soil frost studies. We first parameterize the processes that occur in the spring season by extracting key hydrological events from the long-term time series and analyze the timing across each of these events through ranking. Then, we use stepwise regression to identify the importance of winter and spring season variables for predicting annual streamflow. Together, answers to these questions will illustrate the importance of considering soil frost in headwater catchments.

2. Methodology

2.1. Site description

Our catchments are located within the USDA Forest Service Marcell Experimental Forest (MEF, Lat. 47:31:52 N, Long. 93:28:07 W) near Grand Rapids, Minnesota (USA). The MEF sits on the climatic transition region between areas of seasonally frozen ground and northern boreal regions, and has six peatland dominated catchments that have been under long term observation since 1961 (Sebestyen et al., 2011). The S2 and S5 research catchments are reference basins with central peatlands surrounded by upland forests on mineral soils. Records for these sites include hydrologic, meteorological, and water chemistry

data (Sebestyen et al., 2021b). Minnesota climate is strongly continental with warm, humid summers and cold, dry winters. From 1961 to 2019, mean annual temperature at the catchments was 3.5 °C (Sebestyen et al., 2021b). Average annual temperature has been increasing by 0.4 °C per decade since 1961 with the majority of the warming occurring over the winter months (Sebestyen et al., 2011, January to March, 0.7 °C per decade). Annual precipitation averages 79 cm, with one third of precipitation falling in the form of snow (Sebestyen et al., 2021b). Snow cover in the peatland starts in late October and November and usually lasts until March or April of the following year. There has been no change over time in maximum snow–water equivalent under coniferous and open areas but significant decline under deciduous covers (Sebestyen et al., 2011).

2.1.1. South unit — S2 bog

The S2 watershed has a total size of 9.7 ha which is made up of a 3.2 ha domed peatland encircled by upland forests. The upland vegetation is dominated by aspen (*Populus tremuloides*, *Populus grandidentata*) stands. The peatland is covered by black spruce *Picea mariana* and *Sphagnum* mosses. The bog topography is characterized by a slightly domed peat surface rising 18 cm at its peak with a presumed parallel peatland water table (Richardson et al., 2010). There is a streamflow outlet elevation of 420 m above sea level. Measurements of the peatland WTE are taken near the highest elevation of the bog using a stripchart recorder and daily maximum water table is recorded (Sebestyen et al., 2011). Streamstage is measured using a V-notch weir and strip chart recorder at the South-west end of the catchment (Verry et al., 2018, for data and metadata). Winter snow and frost depth were measured biweekly from 1962 to 2021 starting in February and continuing through snow disappearance (Sebestyen et al., 2021a, for data and metadata). In S2 snow and frost measurements were taken biweekly on two upland snow courses in aspen stands and one bog snow course in a black spruce stand.

2.1.2. North unit — S5 bog

S5 is a larger peatland on the North Unit of the Marcell Experimental Forest that is 52.6 ha in size and contains five small satellite peatlands that drain into a central peatland that is 6.1 ha. The S5 uplands are have some older growth and more diverse with species of aspen, white cedar (*Thuja occidentalis*), white spruce (*Picea glauca*), balsam fir (*Abies balsamea*), pine (*Pinus strobus*, *Pinus resinosa*, *Pinus banksiana*), and mixed hardwoods with an average stand age of 100 years. Bog water table elevations are measured in a similar way as in S2 using stripchart recorders to monitor a central peatland well. Streamstage is measured using a V-notch weir at the Northeast corner of the watershed. Similar to the S2 watershed, snow depth, SWE, and frost depth measurements are taken biweekly in S5 beginning in February and continue through snow disappearance. There are four snow courses in S5, one in an upland clearing with the S5 meteorological station, one in the bog, and two in the uplands (Sebestyen et al., 2011, 2021b).

2.1.3. Forestry sciences laboratory, grand rapids, MN

To increase the temporal resolution and coverage of the snow course data from the MEF, we used supplemental data with a longer record from the USDA Forest Service Grand Rapids Forestry Sciences Laboratory (Lat. 47:14:9.2 N, Long. 93:31:41.9 W), approximately 48 km south of the MEF. Here precipitation, snow inputs, and snow depth are all taken daily from 1915 (precipitation) and 1948 (snow inputs, depth) onwards. A correlation between precipitation inputs at the two sites is shown in Fig. S1. In Grand Rapids the mean annual temperature from 1950 to 2020 was 4.5 °C and precipitation was 71 cm. Snow depth data from 1974–1989 were missing most of the daily values and so these years were removed from the analysis.

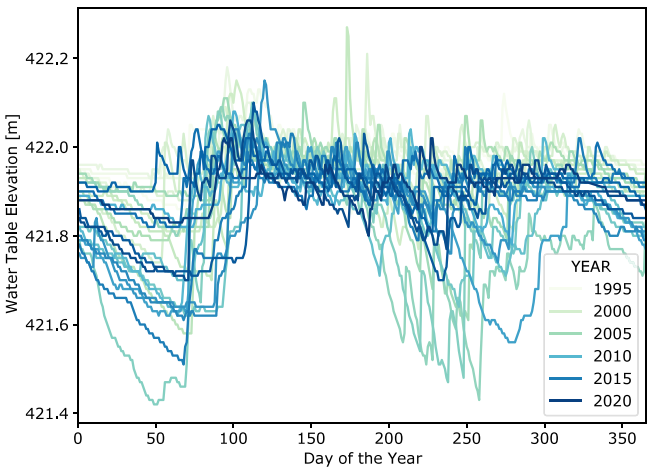

Fig. 1. Daily water table elevation in the S2 bog. Annual water table time series colored by year from 1995 (light green) to 2020 (dark blue). (For interpretation of the references to color in this figure legend, the reader is referred to the web version of this article.)

2.2. Characterizing the timing and magnitude of hydrological events

We first identified hydrological events in the winter and spring periods and derived metrics characterizing two key aspects of these events: magnitude and timing in the water year (defined here as October 1st to September 30th). These standardized metrics can be used to compare hydrological events across multiple years (1995–2020) and detect trends over time. We focused on the winter to spring seasonal transition, because this transition is a period of high flow that often contributes the most to the annual streamflow yield.

The metrics for the snowpack dataset were calculated based on the triangle method used by Trujillo and Molotch (2014) for SWE data. The method, which was developed to identify key snow appearance, disappearance, and peak values for snowpacks in the western United States, has not been applied to snow depth data in Minnesota before. However, annual snow depth time series from Grand Rapids demonstrate a similar triangle structure, so we anticipated that the method will be effective for our needs. Here, we applied the triangle method to the Grand Rapids snow depth data to derive snowpack metrics for both the S2 and S5 catchments. The MEF snowpack data were not used for these metrics because the biweekly data did not have high enough temporal resolution. Implementing this method involved identifying three key dates in the snow season: the date of snow appearance (DOA), the date of peak snow depth (DOP), and the date of snow disappearance (DOD). The DOA and DOD values for each water year were determined to be the first and last non-zero value of snow depth (with a seven-day buffer to control any erratic early or late season snow events). To determine the DOP that best approximates the transition between snow accumulation and ablation, it was necessary to identify first all potential peaks and then investigate the fit to a triangular function for snow depth evolution. To do so, the *find_peaks* function from the *scipy.signal* package in Python 3.8 (Virtanen et al., 2020) was used to first identify all potential peak values between the timing of the 10th and 90th percentile of snow accumulation (to ensure the detected snowpack peak occurred near the middle of the snow season) which had snow depths above half the annual mean. Then, each of the potential peaks was used to simulate snow depth using a triangular function, where snow depth increases linearly from DOA to the date of potential peak, then decreases linearly until it reaches zero at DOD. Each of these fits (with its corresponding DOP) was then compared to the measured snow depth data using a nonparametric Mann–Kendall test for monotonic trends. The DOP whose corresponding fit resulted in the highest correlation coefficient against measured snow depth was

Table 1
Magnitude variables used in the regression model.

Variable	Description	Units
Y_{Flow}	Total annual streamflow, normalized by area	m
$X_{SnowPeak}$	Depth of the snow pack at its peak	cm
X_{MFT}	Maximum thickness of frost	cm
X_{WTE}	Annual average water table elevation	m
$I_{Watershed}$	Watershed, 0 for S2, 1 for S5	–
$X_{AvgTemp}$	Average annual temperature	°C
$X_{TotPrecip}$	Total annual precipitation	cm

selected for that year. The snow depth at DOP was also identified, as well as the duration and rates of the accumulation and melt periods.

For the WTE metrics, we observed that the spring recharge period begins with a typically annual low value right before the spring climb to a seasonal high (Fig. 1). For measuring the magnitude of the spring climb, the overall duration of the recharge period and total WTE recharge of the season were also identified. The *find_peaks* function was again used to select possible dates for the seasonal WTE trough and peak during the spring recharge period. For each of the several possible trough/peak pairs identified, the Mann–Kendall test was again used to compare a linear function of WTE recharge generated against the measured data. The pair with the highest correlation was selected for the timing metrics and their WTE values were recorded.

The spring streamflow timing metrics were selected as the maximum value of the first major peak of the spring season and the timing of first nonzero value as the onset of spring streamflow. The magnitude of the first spring streamflow peak was also recorded. Due to the limited resolution (i.e., biweekly) frost data from the MEF sites, we only identified the maximum frost depth value and date of maximum.

2.3. Rank and correlational analysis

Each timing metric across the data record was examined for annual trends using linear regression across each water year (October 1st–September 30th). This analysis included examining six timing metrics to quantify spring seasonal hydrology: the peak snow depth (S_{peak}), the date of snow disappearance (S_{DOD}), the date of WTE trough (W_{trough}), the date of WTE peak (W_{peak}), the date of streamflow onset (Q_{onset}), and the date of the first streamflow peak (Q_{peak}).

A correlation analysis was used to examine the relationships between the timings of each of the same six variables of interest. For each year, the day of the water year in which these events occurred was recorded in a list and used to rank each of the variables (e.g., if the maximum WTE occurred first among the six events in water year 2012, then it was given rank 1). The ranks for each event were then averaged across all years.

2.4. Multivariate regression

We used multiple regression to examine the interactions among hydrological and climatological variables in controlling streamflow generation in the spring and throughout the year. A stepwise multiple regression model was built to predict the magnitude of total annual streamflow from a set of site-dependent and shared precipitation variables. A total of six predictor variables were used: air temperature ($X_{AvgTemp}$), snowpack depth ($X_{SnowPeak}$), max annual frost thickness (X_{MFT}), average annual WTE (X_{WTE}), total annual precipitation ($X_{TotPrecip}$), and an indicator to designate either the S2 or S5 watershed ($I_{Watershed}$; Table 1). All data used in this model is site-specific. A random sampling of 60% of the years (1995–2020) were used for the stepwise analysis. This subset was then used to build sub-multiple regression models using different combinations of the predictor variables using a stepwise analysis. Each model tested was a subset of the full model, which contains all the predictor variables and all potential combinations of interaction terms. Here $\mathcal{P}()$ is the power set, or all combinations of the interaction term.

$$Y_{Flow} \sim \beta_0 + \mathcal{P}(\beta_{i,j,k,l} X_{i,SnowPeak} X_{j,MFT} X_{k,WTE} I_{l,Watershed}) + \beta_2 X_{AvgTemp} + \beta_3 X_{TotPrecip} \quad (1)$$

A total of 668 sub-models were constructed from the full model shown in Eq. (1). For each model, a second-order bias-corrected Akaike's Information Criterion (AICc) was used to compare predictive capacity, and the models with lower AICc (ΔAICc < 2) were taken as 'candidate' models (Burnham et al., 2011). ΔAICc is the difference between the AICc value of the best fit model and the model of interest. A model with a similar goodness of fit to the best fit model will have a minimized ΔAICc. Each candidate model was then used to predict the remaining 40% of the data set and validated for linearity, constant variance, and normality. In addition, each model was given a weight, W_i, which is the probability of the model given the data (Burnham et al., 2011). W_i is computed as the likelihood of a given model over the total number of models and can be read as "the probability of model i is w_i". For each predictor variable, these weights were summed across the sub-models containing that particular predictor variable to obtain the overall relative importance of each variable. This process was then repeated 1000 times with a different random sampling of years for each candidate model to determine an expected range of RMSE. This processes was repeated to predict the magnitude of the first spring streamflow peak, Q_{Peak}, which is outlined in the supplementary materials.

To further evaluate the results from the variable importance analysis, a separate dominance analysis was run to determine the independent effects of each predictor variable within the best fit model (Budescu, 1993; Murray and Conner, 2009). This method allowed us to consider the amount of variation in the annual streamflow data that is explained by each individual predictor variable while removing any covariance between predictors. It is a metric of the relative explanatory power of each variable *within* a single model. This dominance analysis is different then the step-wise regression model analysis which determines variable importance *between* models. The dominance analysis was run using all of the data, not only the 60% random sampling.

3. Results

Total annual streamflow, normalized by respective catchment areas, decreased in S2 at a rate of 1.9 cm per water year over 25 years ($p < 0.005$, 1995–2020) and in S5 at a rate of 2.9 cm per water year also over 25 years ($p < 0.05$, Fig. 2a). The decrease in annual streamflow occurred despite no statistically significant changes in snowfall fraction ($p = 0.69$; Fig. 2b), annual precipitation ($p = 0.331$), snowfall inputs ($p = 0.829$), or winter air temperature ($p = 0.47$; Fig. 2c). There was an increase in mean annual air temperature of 0.4 °C per decade ($p = 0.0005$, Sebestyen et al. (2011)), but annual streamflow across multiple years shows no statistically significant correlation with mean annual air temperature ($p = 0.775$). Average annual WTE in the S2 peatland decreased at a rate of 4 cm/decade ($p = 0.002$) with the trough WTE decreasing at a slightly faster rate of 6.5 cm/decade ($p = 0.066$).

3.1. Streamflow generation

Results from the signal processing of hydrological data showed a consistent sequence of events as water traveled from the snowpack through the landscape to generate streamflow. Fig. 3 shows the relationship between the streamflow and WTE in S2 and S5. First, there is a clear WTE threshold that dictates the initiation of streamflow in both S2 and S5 (Fig. 3a–b), which demonstrates the surface water storage must first be "filled" before it "spills" into the stream. There is also a direct and statistically significant relationship between the timing of peak WTE and the first streamflow peak in both catchments across years (Fig. 3c – d).

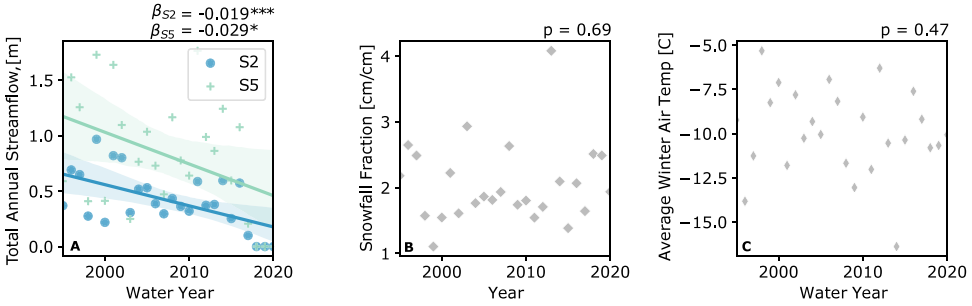

Fig. 2. (A) Summary of decreasing annual streamflow trends in S2 and S5 at the MEF, (B) lack of snow or precipitation trends from the Grand Rapids meteorological station, and (C) lack of winter air temperature trends from the MEF meteorological station (Dec. 1st–March 31st). β values in (A) show the rate of water table change over time in S2 and S5. P-values show the insignificance of the annual trends in (B) and (C). Stars indicate the level of significance for each trend with '***' denoting p < 0.001 and '*' denoting p < 0.05. Shaded areas indicate a 95% confidence interval.

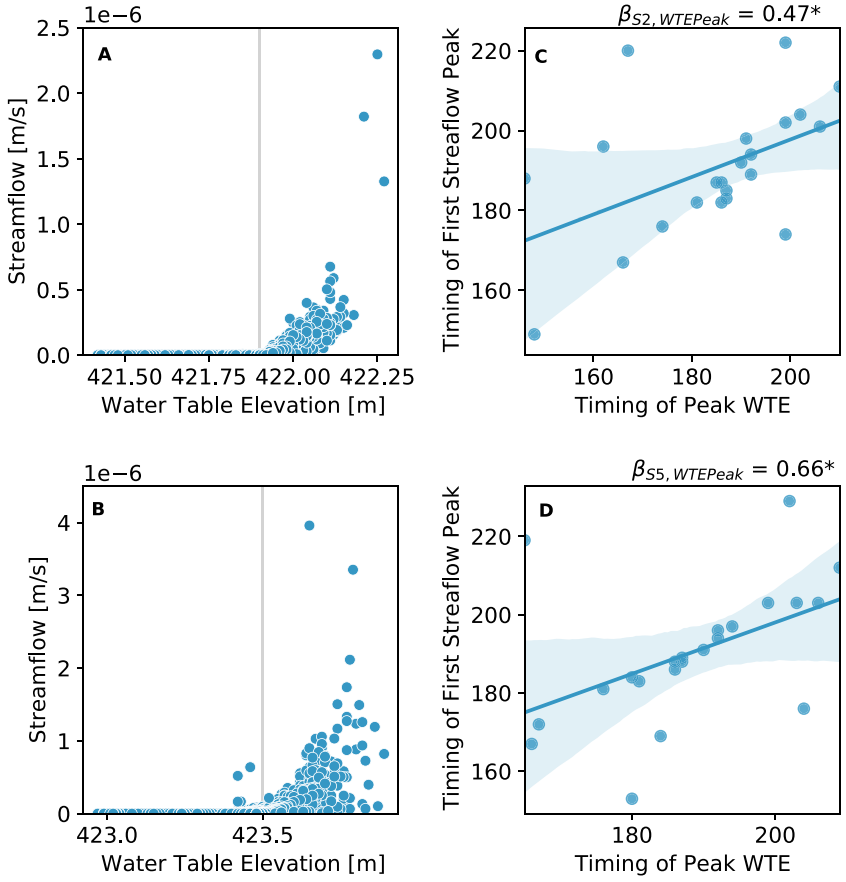

Fig. 3. The non-linear relationship between water table elevation (WTE) and streamflow. (A – B) The thresholds for streamflow initiation in S2 and S5 respectively, shown at the daily time scale. (C–D) Show the relationship between the timing of peak WTE and the first detected streamflow peak in S2 and S5 respectively. β values are the slopes of the relationships in (C) and (D). The statistical significance of the relationships is shown using '*' to represent p < 0.05. Shaded areas indicate a 95% confidence interval.

Fig. 4 shows the ranked estimates for the timing of each hydrological event for 2013 (top panel) and for all years of record (bottom panel). When averaged across years and catchments, dates of S_{peak}, W_{trough}, Q_{onset}, S_{DOD}, W_{peak}, and Q_{peak} occurred sequentially with mean dates of 135, 156, 166, 170, 187, and 190 respectively. Dates for WTE trough (W_{trough}) and peak (W_{peak}) were similar in S2 and S5, with S5 showing more variation in trough dates and less variation in peak dates than S2. Streamflow onset (Q_{onset}) in S5 typically occurred later than in S2 and with much higher temporal variation (mean 164.7 and 168; SD of 14.8 and 21.7 respectively). Date of first streamflow peak (Q_{peak}) was similar for both catchments, 190.4 and 190.1 respectively. While there is a clear sequence of events during spring, the timing for most of the individual events is not correlated (with the exception of Q_{peak} and W_{trough} as shown in Fig. 3). For instance, the timing of peak snow, the timing of the WTE trough, and the timing of streamflow onset are not correlated (Fig. S4).

3.2. Relative impacts of landscape controls on streamflow

The stepwise regression model (Eq. (1)) was used to determine the relative explanatory power of each hydrological and climatological input variable on annual streamflow. Select model candidates (smallest values of ΔAICc) for predicting the total annual flow are shown in Table 2. The base model was ranked last of the 668 models with the highest ΔAICc. Also listed are K, the degrees of freedom in the selected model, and w_i, or the probability of the model given the data. Of the metrics shown in Table 2, the value of w_i, or weight, is the

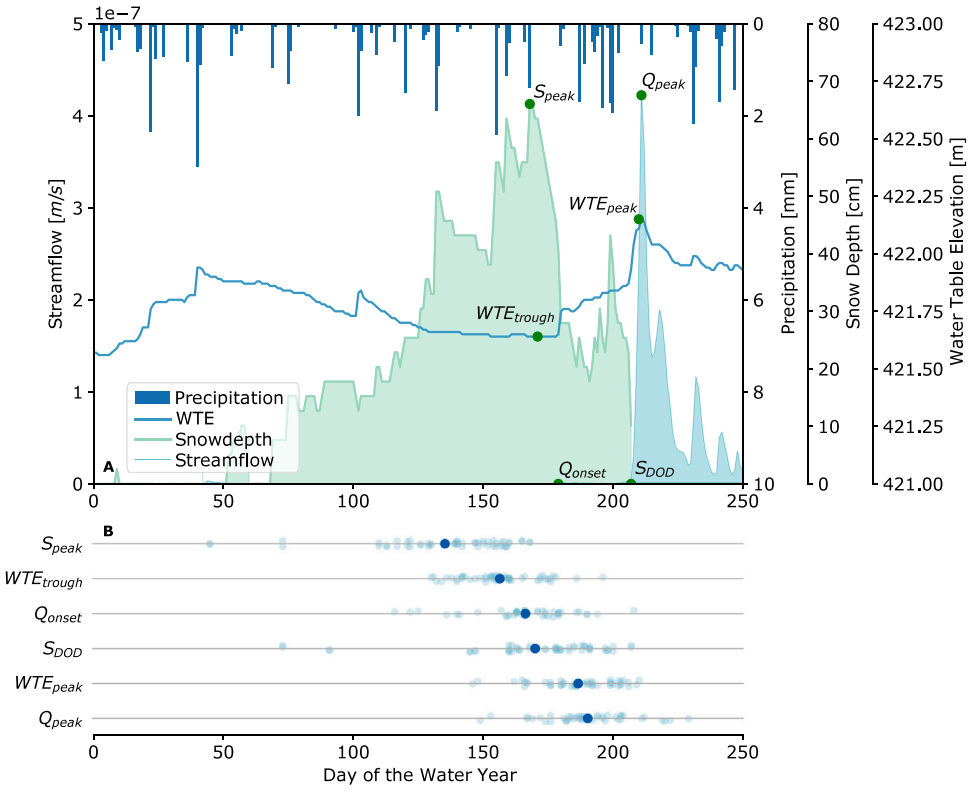

Fig. 4. Hydrologic cascade from snowfall to streamflow. (A) A sample year, 2013, showing each data element overlayed with critical points derived using the parameterization methods. (B) Annual trends in the derived statistics for magnitude compiled over both catchments. Dark blue dots show the average date of occurrence for each metric over the time period from 1995–2020. The water year is defined as October 1st through September 31st of the following Gregorian calendar year.

most important as it shows the probability that of all of the models considered, that model is the best model for making predictions.

Each model in Table 2 shows zero mean and standardized residuals, but all of the candidate models also show a slight increasing trend in the variance as a function of the residuals, which may violate the constant variance assumption. The direction of the increase is not consistent. Using Cook's distance (1 > distance > 0.5), discharge in Model 3 for year 2013 and S2 was identified as an outlier (Cook, 2000). All other models show no outliers. The remaining validation years were then used to predict values of total annual flow and compare to the observed flows from the same year. Sample plots of these values are shown in Fig. 5.

Frost was an important predictor in the summed weights for each of the predictor variables (Fig. 5). The individual variables (top four rows) showed the highest importance, with maximum frost thickness being the most highly weighted variable with a weight of 0.98 out of a possible normalized score of 1, meaning that frost had the most additive predictive power when present in a model. Mean frost thickness in S2 was 5.7 cm with a range of 0 to 36 cm (1995–2020). In S5, mean frost thickness is 10.5 cm with a range of 0 to 42 cm. The date of maximum frost at S5 occurred later in the season when compared to S2, and when ranked with other spring variables, occurred last. Total annual precipitation was ranked as the second most important predictor variable. However, when the dominance analysis is used on the top model, $Y_{Flow,1}$, only 12.3% of the total variance explained by the model is explained by the maximum frost thickness. 49.4% of the total variance is explained by the water table elevation, 26% by precipitation, and 12.3% by the frost thickness and water table interaction term. When regression was also applied to predict the magnitude at Q_{peak}, shown in Tables S1 and S2 of the supplementary materials, snow depth was the most highly weighted variable (0.971) followed closely by maximum frost depth (0.923). Within the top weighted model, however, it was the snow depth and catchment interaction term that was describing the majority of the variance (42.9%) followed by catchment (34.8%), maximum frost thickness (17.5%), and then snow depth (4.8%). As a result, while frost may have a large weight when each model is considered as a whole during the step-wise regression analysis, frost is not always the most important variable within each model. (see Fig. 6).

Additionally, of the models tested with only a single predictor, the model with WTE had the most predictive power with a ΔAICc of 14.25 followed successively by the models with the catchment indicator (ΔAICc 15.25), average annual temperature (ΔAICc 25.11), total annual precipitation (ΔAICc 26.03), maximum frost thickness (ΔAICc 29.58), and finally peak snow depth (ΔAICc 31.38). Catchment indicator is high in these rankings because of the high correlation between catchment and average WTE. This result, and the results from the dominance analysis, suggest that frost is not the singular best indicator of streamflow, but is an important predictor in the context of other better streamflow predictors like precipitation and WTE.

From the candidate models, it is important to note the interchangeability of WTE and catchment. Because the average WTE in S2 is lower than S5 (421 m vs. 423 m), WTE acts as a pseudo indicator variable for catchment but there is a slight dominance of WTE over catchment. For example the top two models in Table 2 are the same components other than the presence of either X_{WTE} variables in $Y_{Flow,1}$ or $I_{Watershed}$ in $Y_{Flow,2}$. Additionally, X_{WTE} has a slightly higher weight than $I_{Watershed}$ (Fig. 5).

4. Discussion

We examined the interactions among climatological and hydrological drivers of streamflow in snow-dominated catchments. Using long-term data from two headwater catchments at the Marcell Experimental Forest in northern Minnesota (S2 and S5), our analysis showed that the annual streamflow decreased between 1995 and 2017, with S5 decreasing at a faster rate than S2. In fact, S5 has shown little to no

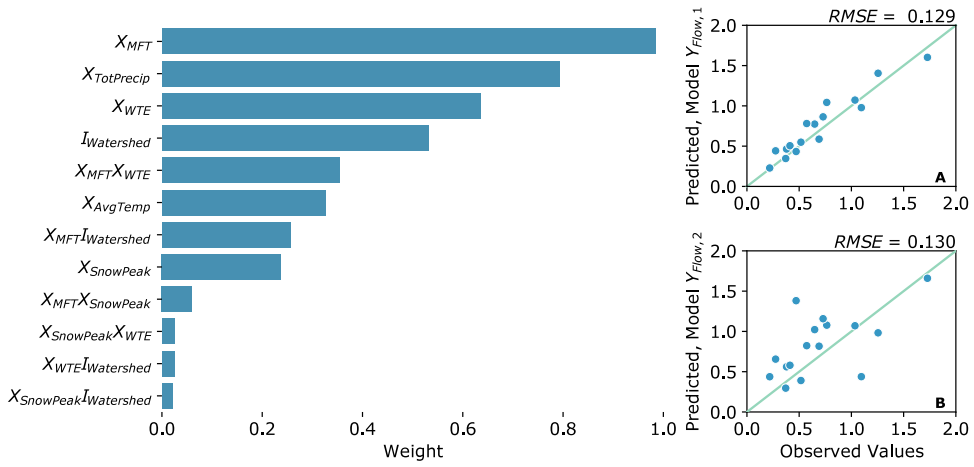

Fig. 5. Model results showing: Left, variable importance from the stepwise regression model. Terms of order 3 or higher have been removed because of insignificance (summed weight = 0) (A–B) show a sample of two observed models from candidate model $Y_{Flow,1}$ and $Y_{Flow,2}$ with the minimum RMSE values from all 1000 iterations. Green line shows the one to one relationship.

Table 2
Selected models for total annual streamflow in order of AICc.

Model	K	AICc	ΔAICc	Weight
$Y_{Flow,1} \sim \beta_0 + \beta_1 X_{MFT} + \beta_2 X_{WTE} + \beta_3 X_{TotPrecip} + \beta_4 X_{MFT} X_{WTE}$	6	5.13	0	0.16
$Y_{Flow,2} \sim \beta_0 + \beta_1 X_{MFT} + \beta_2 X_{Watershed} + \beta_3 X_{TotPrecip} + \beta_4 X_{MFT} X_{Watershed}$	6	5.84	0.71	0.11
$Y_{Flow,3} \sim \beta_0 + \beta_1 X_{MFT} + \beta_2 X_{Watershed} + \beta_3 X_{TotPrecip}$	5	7.07	1.94	0.06
$Y_{Flow,4} \sim \beta_0 + \beta_1 X_{MFT} + \beta_2 X_{WTE} + \beta_3 X_{TotPrecip}$	5	7.08	1.96	0.06
$Y_{Flow,5} \sim \beta_0 + \beta_1 X_{MFT} + \beta_2 X_{WTE} + \beta_3 X_{TotPrecip} + \beta_4 X_{MFT} X_{WTE} + \beta_5 X_{AvgTemp}$	7	7.95	2.82	0.04
...				
$Y_{Flow} \sim \beta_0 + \beta_1 X_{SnowPeak} X_{MFT} X_{WTE} I_{Watershed} + \beta_2 X_{AvgTemp} + \beta_3 X_{TotPrecip}$	19	111.2	106.06	1.50E−24

streamflow out of the peatland in the last 4 years of the record. These declining streamflow trends showed a small significant correlation ($p = 0.044$) with maximum annual snowpack (Fig. S3) but no significant correlation with various other climatic variables such as snowfall fraction (Fig. 2b) and winter air temperature (Fig. 2c). This lack of correlation suggests that the observed changes in streamflow must be considered in conjunction with other land surface drivers. One possible driver may be an increase in evapotranspiration caused by increases in surface energy and air temperature (Badger et al., 2021). However, there is no correlation between air temperature and streamflow ($p > 0.5$), which means that while increasing evapotranspiration is still a possible cause, it likely is not the whole explanation (we could not perform direct analysis with respect to ET since direct measurements of ET are not available). Instead, we hypothesize that the decrease in streamflow is a result of the shifts in both hydrological connectivity within the wetlands and how this connectivity regulates the streamflow generation processes. By exploring the role of other climatological and hydrological drivers within the peatland catchments, our results illustrate the complex relationships between snow, water table elevations, and streamflow, as well as the important role of soil frost in controlling these relations.

4.1. Hydrologic connectivity

Our results show that within peatland catchments, there is a clear connection between WTE and streamflow, where the shift in peak WTE towards later in the spring induces a parallel shift in the first streamflow peak (Fig. 3). This coupling between WTE and streamflow highlights the importance of hydrological connectivity within this system. Due to the elevated WTE in the spring compared to the rest of the year (Fig. 1), this coupling also identifies the spring season as the most important part of the year for dictating annual streamflow magnitude.

This hydrologic connectivity is also supported by the ranking analysis from Fig. 4 which gives the sequence of events that lead to streamflow generation from the snowpack (Fig. 4). The first event in the ordering is the timing of the peak snowpack, indicating the beginning of the snow melt season. The second event is the timing of the lowest point in the WTE, the trough, which precedes recharge. There is a delay between these first two events potentially due to peatland storage, the refreezing of water into the snowpack as it melts (Heldmyer et al., 2021), ripening of the snowpack, or sublimation of snow back to the atmosphere. Once the water has begun reaching the peatland water table, the ranking scheme indicates that the water table then acts as a secondary storage system until streamflow initiates. Streamflow onset is then initiated only after the WTE rises above a threshold relative to the outlet stream elevation (Fig. 3a–b).

The date of frost disappearance was excluded from this ranking because of the low data resolution for frost depth, so the timing of soil frost in relation to water table recharge and streamflow onset is unknown. Past studies that have found no dependence between frost and streamflow timing have shown this is likely due to the frost thawing before recharge begins (Lindström et al., 2002), while other sites that have shown dependence between streamflow and soil frost have identified rapid streamflow response when precipitation is falling on frozen snow-free ground (Shanley and Chalmers, 1999). For our results to be put into context of these previous studies, higher frequency soil frost monitoring is needed.

4.2. Explanatory power of soil frost

Although the role of soil frost disappearance timing remains uncertain, the stepwise multiple regression model built to predict streamflow from both climatological and hydrological variables demonstrated a strong dependence on soil frost thickness. The five best performing models for streamflow each contains a combination of frost thickness, water table elevation, catchment, air temperature, and total annual precipitation. Peak snowpack depth at the MEF is not selected as an important predictive variable in these top models, which was unexpected,

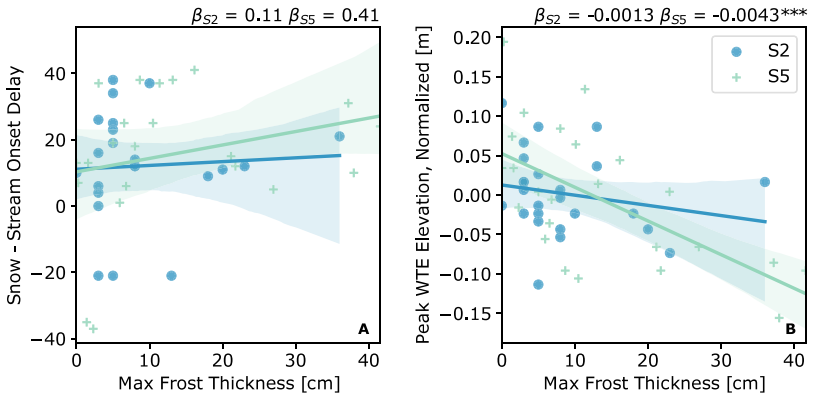

Fig. 6. (A) Snow-Stream Onset Delay (Date of Stream Onset–Date of Peak Snow at MEF) as controlled by frost thickness. (B) Peak WTE, normalized by average WTE in each catchment, as a function of frost thickness. Beta values show the slopes for each relationship. Stars indicate the level of significance for each trend with '***' denoting $p < 0.001$. Shaded areas indicate a 95% confidence interval.

given that past studies commonly use SWE to predict streamflow (Bayard et al., 2005; Ryberg et al., 2016). However, in our case, snow depth may not capture the same temporal variability in snow density as SWE, limiting the ability to predict spring streamflow from snow depth.

Maximum frost thickness is the most highly weighted predictor variable when compared to all other possible predictors (with weight defined in Section 2.4). This result runs counter to the expectation that precipitation or snowpack, the more commonly used predictors for streamflow, would have the most weight. Total annual precipitation was the second highest weighted predictor followed by both WTE and catchment. However, it is important to note two things. First, when each of the predictor variables are used to predict streamflow on their own, maximum frost thickness has the second lowest explanatory power. Second, within the best model for streamflow, frost was only describing 12% of the total model variance. Similar to snowpack, soil frost is not present every year, and therefore should not be directly relied upon to solely predict streamflow. Instead, in areas where frost may appear, it should be considered as an important driver of streamflow generation and a supporting predictor for streamflow amount.

This result is not unexpected, given the wealth of data showing the influence of soil frost on infiltration in both modeled soil columns (Zhao and Gray, 1999) and catchments on short time scales (< 3 years, Shanley and Chalmers (1999)). Nevertheless, it reinforces the idea that frost is an important hydrologic factor even across long time scales. Additionally, while many of these analyses have looked at the effects of soil frost on infiltration or streamflow (Ala-Aho et al., 2021; Bayard et al., 2005; Lindström et al., 2002), our results show *how* these effects extend to streamflow, lateral dynamics, and connective fluxes across the catchment. Specifically, in areas where the season of frozen ground overlaps with the spring recharge season, as does in much of northern North America, soil frost is sometimes a dominant factor affecting both the timing and magnitude of recharge and streamflow in forested catchments. While it is unclear why soil frost seems to be particularly influential in our studied catchments compared to forested catchments (Aho et al. 2021), one reason may be that the perched water table may make peatlands more susceptible to higher frost contents in the upper ground layers. Higher frost content in the upper layers would cause more drastic restrictions in infiltration and a larger fraction of snowmelt being routed to streamflow.

4.3. Applications to water balance partitioning

The presence of increased soil frost depth is generally known to either limit the infiltration of water to the water table, making the recharge and baseflow processes slower and delaying streamflow initiation, or limit recharge altogether and cause rapid streamflow generation through overland flow (Ala-Aho et al., 2021; Fuss et al., 2016; Shanley and Chalmers, 1999). These processes dictate the division of water between that which is available to plants for transpiration, and that which flows to streams. While the effects of different plant cover types, soil types, and snow cover distributions on water partitioning have been studied (Hammond et al., 2019), the coupled effects of soil frost on partitioning are still understudied. In this section we present several hypotheses and preliminary results to illustrate how frost could control snowmelt partitioning.

In the MEF catchments, the decoupled timing between snowpack melt and streamflow initiation implies that there may be an influence of frost on this partitioning in both S2 and S5. Fig. 7 shows a depiction of how different snowfall and winter temperature scenarios may dictate (i) the depth of the frost layer and (ii) the partitioning of SWE for spring streamflow and evapotranspiration. In each proposed scenario, data from the S2 and S5 catchments (1995–2020) have been divided into each of four winter temperature and snowfall scenarios. Years with winter temperatures above the average are considered 'warmer winter' and years with snowfall totals above the average are considered 'more snowfall' (and vice versa). Scenario A shows the baseline conditions at the MEF where there is more snowfall and colder winter temperatures compared to future projected conditions. In this scenario, a large snowpack and colder temperatures result in a lower maximum frost thickness compared to a deeper frost depth in scenario B (see light blue boxplots in upper row), where there is little snow and less insulation, or the thin frost layer in C where there are warmer temperatures. Because of the deeper snowpacks, scenarios A and C will have more water available than in scenarios B and D respectively (Fig. 7, dark blue areas in the arrows).

Snow–water equivalent represents the amount of water that is available to recharge soil storage or runoff to spring streamflow, thus less SWE can result in a reduction in overall streamflow water availability (Barnett et al. (2005) ; Fig. 7A to B, or C to D, purple arrows and boxplots). Additionally, the depth of soil frost may control the partitioning of SWE over two steps: first, by controlling the amount of soil water availability in early spring, and then, the amount of soil water taken up by evapotranspiration in the late spring. In the first stage, the presence of frost limits early snowmelt infiltration and enhances surface runoff to streamflow, but we hypothesize that a reduction in vertical drainage may also increase saturation in the top part of the peat soil column. In the second stage, transpiration is assumed to start only after the ground has thawed and after leaf out (Mellander et al., 2006). Here, because the melting of the frost layer depends on the insulation effects of snow, snow also plays a role in determining the timing of transpiration onset. Therefore, the magnitude of spring evapotranspiration will depend both on the timing of soil frost disappearance and the amount of soil frost. For example, in scenario A, there is a large amount of water available in the snowpack, and because of the deep frost layer coupled with

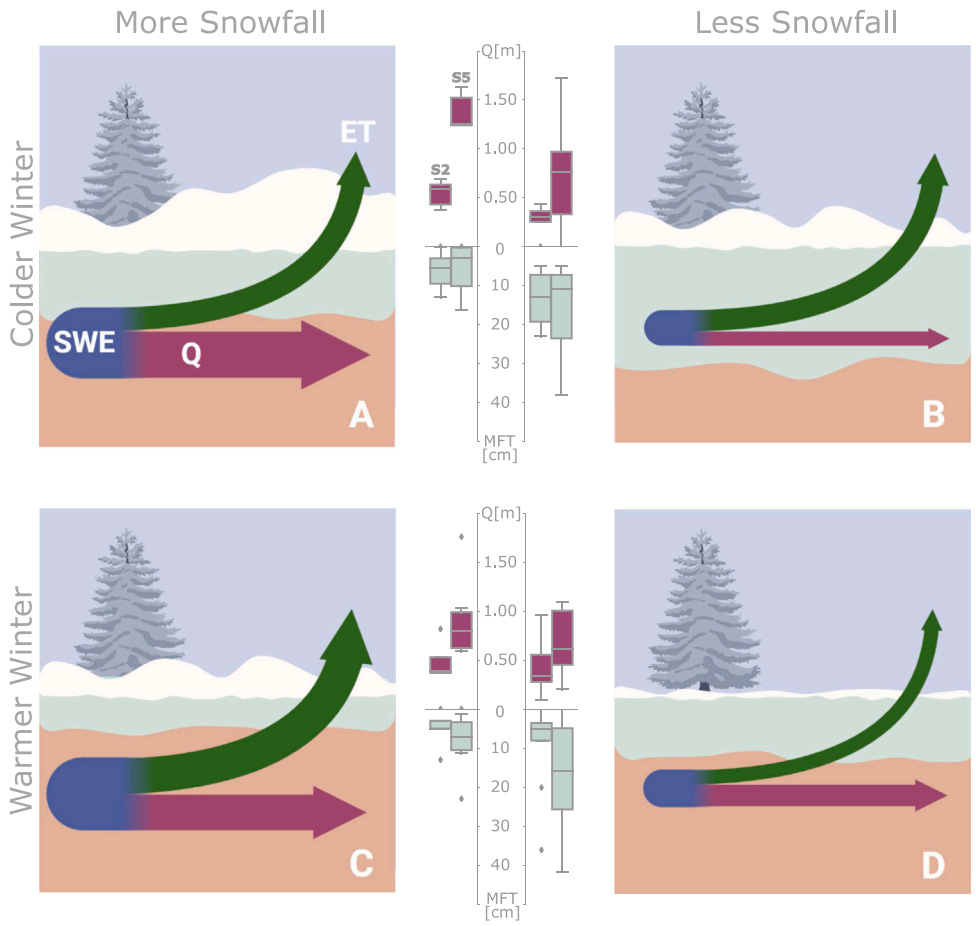

Fig. 7. Conceptual diagram representing the effects that frost could have on the partitioning of precipitation into evapotranspiration and annual streamflow during and after snowmelt. Light blue shading represents frost depth. Relative magnitude of SWE due to snowfall is shown in dark blue. SWE splits into diverging arrows to show the relative partition between evapotranspiration (dark green) and streamflow (purple) respectively. The center column shows frost depth data (light blue) and total annual streamflow data (purple) from the MEF partitioned into each of the four scenarios. Deep vertical drainage, though known to occur in S2 and S5 (Verry et al., 2011), is not depicted for simplicity. (For interpretation of the references to color in this figure legend, the reader is referred to the web version of this article.)

the deep snowpack, more of the water is lost to overland flow due to inhibited infiltration and delayed transpiration onset (therefore Q in A > Q in C and ET in A < ET in C despite the same snowfall inputs). However, comparing scenario B to A, there is a thicker frost layer, as confirmed by the MEF data, but a larger fraction of the available water is directed towards evapotranspiration because the frost layer melts out more quickly due to the small snowpack, leaving more time for transpiration in the spring. This is reflected in the data from S2 and S5 which respectively show a lower amount of annual streamflow in scenario B compared to scenario A. There is also a lot more variation in the data during the years with less snowfall, likely due a patchy snow cover.

This redistribution of soil water storage towards earlier spring evapotranspiration with deep frost and little snowfall could lead to overall increases in the evaporative fraction of meltwater inputs. We can see that if winter temperatures increase and snowfall rates stay constant (A ⟶ C), there may actually be overall increase in evapotranspiration at the expense of streamflow. If winter temperatures remain constant but snowfall decreases (A ⟶ B) the rates of evapotranspiration may remain relatively constant despite the decrease in water availability, because of the shift in partitioning due to frost. If there are simultaneous increases in temperature and decreases in snowfall (A ⟶ D) the partition remains relatively the same. Accordingly, we could observe decreases in both evapotranspiration rates and overland runoff. Therefore, it is important to consider the interactions of snow, frost, and water table dynamics, when determining SWE partitioning in headwater catchments like the MEF.

5. Conclusions

Our results demonstrated the hydrologic connectivity between the snowpack, water table, frost, and streamflow during the winter–spring transition, and highlights the importance of frost in streamflow generation in peatlands. This research shows that in the context of catchment management, it is important to monitor the snow pack and the frost layer. Together, the interactions between snow and frost give a more holistic understanding of streamflow generation. These interactions need to be properly accounted for in hydrological and land surface models, so that we can improve our abilities to predict long-term catchment response to environmental change and improve water management.

6. Open research

All data used in this paper is accessible online at the following locations:

- **MEF precipitation**: Sebestyen, S.D., D.T. Roman, J.M. Burdick, N.K. Lany, R.L. Kyllander, A.E. Elling, E.S. Verry, and R.K. Kolka. 2021. Marcell Experimental Forest daily precipitation, 1961 — ongoing ver 2. Environmental Data Initiative. https://doi.org/10.6073/pasta/61c7154b78f521841ff8e25fc6db9987
- **MEF soil frost**: Sebestyen, S.D., E.S. Verry, A.E. Elling, R.L. Kyllander, D.T. Roman, J.M. Burdick, N.K. Lany, and R.K. Kolka. 2020. Marcell Experimental Forest biweekly bog frost depth, 1985

— ongoing ver 1. Environmental Data Initiative. https://doi.org/10.6073/pasta/0f184840135054ab017c8aad6496c353

- **MEF snow and SWE:** Sebestyen, S.D., J.M. Burdick, D.T. Roman, N.K. Lany, R.L. Kyllander, A.E. Elling, E.S. Verry, and R.K. Kolka. 2021. Marcell Experimental Forest biweekly snow depth, frost depth, and snow–water equivalent, 1962 — ongoing ver 2. Environmental Data Initiative. https://doi.org/10.6073/pasta/2ff0a9c2cce5a130b7b51fefe7ff38c6
- **MN DNR snow and SWE:** Courtesy of the Minnesota Department of Natural Resources Grand Rapids Forestry Lab - Station 213303. Data available here: https://www.dnr.state.mn.us/climate/historical/daily-data.html
- **MEF streamflow**: Verry, Elon S.; Elling, Arthur E.; Sebestyen, Stephen D.; Kolka, Randall K.; Kyllander, Richard. 2018. Marcell Experimental Forest daily streamflow data. Fort Collins, CO: Forest Service Research Data Archive. https://doi.org/10.2737/RDS-2018-0009
- **MEF WTE:** Sebestyen, S.D., J.M. Burdick, D.T. Roman, N.K. Lany, R.L. Kyllander, A.E. Elling, E.S. Verry, and R.K. Kolka. 2021. Marcell Experimental Forest daily peatland water table elevation, 1961 — ongoing ver 2. Environmental Data Initiative. https://doi.org/10.6073/pasta/2a75c323256252a763e9343f0df7b6af

CRediT authorship contribution statement

Mariel W. Jones: Conceptualization, Formal analysis, Data curation, Writing – original draft, Writing – review & editing, Funding acquisition. **Stephen D. Sebestyen:** Writing – review & editing, Funding acquisition. **Salli F. Dymond:** Writing – review & editing. **G.H. Crystal Ng:** Writing – review & editing, Funding acquisition. **Xue Feng:** Conceptualization, Writing – review & editing, Funding acquisition.

Declaration of competing interest

The authors declare the following financial interests/personal relationships which may be considered as potential competing interests: Dr. Stephen D. Sebestyen reports financial support was provided by USDA Forest Service Northern Research Station. co-author serves as a guest editor to the JoH Women in Hydrology Special Issue - X.F.

Data availability

Published data sources are made available at the end of the document.

Acknowledgments

M.J. and X.F. were supported by the Department of Energy Environmental System Science, United States grant DE-SC0019036. The long-term monitoring at the MEF and the contributions of S.D.S are funded by the Northern Research Station of the USDA Forest Service, United States.

Appendix A. Supplementary data

Supplementary material related to this article can be found online at https://doi.org/10.1016/j.jhydrol.2022.128801.

Supplementary information contains a maps of the referenced sites and additional model results for peak water table elevation.

References

Ala-Aho, P., Autio, A., Bhattacharjee, J., Isokangas, E., Kujala, K., Marttila, H., Menberu, M., Meriö, L.-j., Postila, H., Rauhala, A., Ronkanen, A.-k., Rossi, P.M., Saari, M., Torabi Haghighi, A., Kløve, B., 2021. What conditions favor the influence of seasonally frozen ground on hydrological partitioning? A systematic review. Environ. Res. Lett. 16, 43008. http://dx.doi.org/10.1088/1748-9326/abe82c.

Alexander, R.B., Boyer, E.W., Smith, R.A., Schwarz, G.E., Moore, R.B., 2007. The Role of Headwater Streams in Downstream Water Quality. J. Am. Water Res. Assoc. 43 (1), 41–59. http://dx.doi.org/10.1111/j.1752-1688.2007.00005.x, www.blackwell-synergy.com.

Aygün, O., Kinnard, C., Campeau, S., 2019. Impacts of climate change on the hydrology of northern midlatitude cold regions:. 44 (3), 338–375. http://dx.doi.org/10.1177/0309133319878123, https://Doi-Org.Ezp1.Lib.Umn.Edu/10.1177/0309133319878123.

Badger, A.M., Bjarke, N., Molotch, N.P., Livneh, B., 2021. The sensitivity of runoff generation to spatial snowpack uniformity in an alpine watershed: Green lakes valley, niwot ridge long-term ecological research station. Hydrol. Process. 35 (9), http://dx.doi.org/10.1002/hyp.14331, https://onlinelibrary.wiley.com/doi/10.1002/hyp.14331.

Barnett, T.P., Adam, J.C., Lettenmaier, D.P., 2005. Potential impacts of a warming climate on water availability in snow-dominated regions. Nature 438 (7066), 303–309. http://dx.doi.org/10.1038/nature04141, http://www.nature.com/articles/nature04141.

Bayard, D., Stähli, M., Parriaux, A., Flühler, H., 2005. The influence of seasonally frozen soil on the snowmelt runoff at two Alpine sites in Southern Switzerland. J. Hydrol. 309 (1–4), 66–84. http://dx.doi.org/10.1016/j.jhydrol.2004.11.012, https://linkinghub.elsevier.com/retrieve/pii/S0022169404005633.

Berghuijs, W.R., Woods, R.A., Hrachowitz, M., 2014. A precipitation shift from snow towards rain leads to a decrease in streamflow. Nature Clim. Change 4 (7), 583–586. http://dx.doi.org/10.1038/nclimate2246.

Bridgham, S.D., Cadillo-Quiroz, H., Keller, J.K., Zhuang, Q., 2013. Methane emissions from wetlands: Biogeochemical, microbial, and modeling perspectives from local to global scales. Global Change Biol. 19 (5), 1325–1346. http://dx.doi.org/10.1111/gcb.12131, https://onlinelibrary.wiley.com/doi/10.1111/gcb.12131.

Budescu, D.V., 1993. Dominance analysis: A new approach to the problem of relative importance of predictors in multiple regression.. Psychol. Bull. 114 (3), 542–551. http://dx.doi.org/10.1037/0033-2909.114.3.542, http://doi.apa.org/getdoi.cfm?doi=10.1037/0033-2909.114.3.542.

Burnham, K.P., Anderson, D.R., Huyvaert, K.P., 2011. AIC model selection and multimodel inference in behavioral ecology: Some background, observations, and comparisons. Behav. Ecol. Sociobiol. 65 (1), 23–35. http://dx.doi.org/10.1007/s00265-010-1029-6, http://link.springer.com/10.1007/s00265-010-1029-6.

Cohen, M.J., Creed, I.F., Alexander, L., Basu, N.B., Calhoun, A.J.K., Craft, C., D'Amico, E., DeKeyser, E., Fowler, L., Golden, H.E., Jawitz, J.W., Kalla, P., Kirkman, L.K., Lane, C.R., Lang, M., Leibowitz, S.G., Lewis, D.B., Marton, J., McLaughlin, D.L., Mushet, D.M., Raanan-Kiperwas, H., Rains, M.C., Smith, L., Walls, S.C., 2016. Do geographically isolated wetlands influence landscape functions? Proc. Natl. Acad. Sci. 113 (8), 1978–1986. http://dx.doi.org/10.1073/pnas.1512650113, www.pnas.org/cgi/doi/10.1073/pnas.1512650113 http://www.pnas.org/lookup/doi/10.1073/pnas.1512650113.

Colvin, S.A.R., Sullivan, S.M.P., Shirey, P.D., Colvin, R.W., Winemiller, K.O., Hughes, R.M., Fausch, K.D., Infante, D.M., Olden, J.D., Bestgen, K.R., Danehy, R.J., Eby, L., 2019. Headwater Streams and Wetlands are Critical for Sustaining Fish, FisherIes, and Ecosystem Services. American Fisheries Service Special Report, Vol. 44, (2), pp. 73–91. http://dx.doi.org/10.1002/fsh.10229, www.fisheries.org, https://onlinelibrary.wiley.com/doi/10.1002/fsh.10229.

Cook, R.D., 2000. Detection of influential observation in linear regression. Technometrics 42 (1), 65–68. http://dx.doi.org/10.1080/00401706.2000.10485981, https://www.tandfonline.com/action/journalInformation?journalCode=utch20.

Feng, X., Deventer, M.J., Lonchar, R., Ng, G.H.C., Sebestyen, S.D., Roman, D.T., Griffis, T.J., Millet, D.B., Kolka, R.K., 2020. Climate sensitivity of peatland methane emissions mediated by seasonal hydrologic dynamics. Geophys. Res. Lett. 47 (17), 1–9. http://dx.doi.org/10.1029/2020GL088875.

Ford, C.M., Kendall, A.D., Hyndman, D.W., 2020. Effects of shifting snowmelt regimes on the hydrology of non-alpine temperate landscapes. J. Hydrol. 590 (March), 125517. http://dx.doi.org/10.1016/j.jhydrol.2020.125517.

Foster, L.M., Bearup, L.A., Molotch, N.P., Brooks, P.D., Maxwell, R.M., 2016. Energy budget increases reduce mean streamflow more than snow-rain transitions: Using integrated modeling to isolate climate change impacts on Rocky Mountain hydrology. Environ. Res. Lett. 11, 44015. http://dx.doi.org/10.1088/1748-9326/11/4/044015.

Fuss, C.B., Driscoll, C.T., Green, M.B., Groffman, P.M., 2016. Hydrologic flowpaths during snowmelt in forested headwater catchments under differing winter climatic and soil frost regimes. Hydrol. Process. 30 (24), 4617–4632. http://dx.doi.org/10.1002/hyp.10956, https://onlinelibrary-wiley-com.ezp3.lib.umn.edu/doi/full/10.1002/hyp.10956.

Golden, H.E., Sander, H.A., Lane, C.R., Zhao, C., Price, K., D'Amico, E., Christensen, J.R., 2016. Relative effects of geographically isolated wetlands on streamflow: A watershed-scale analysis. Ecohydrology 9 (1), 21–38. http://dx.doi.org/10.1002/eco.1608, https://onlinelibrary.wiley.com/doi/10.1002/eco.1608.

Gorham, E., 1991. Northern peatlands: Role in the carbon cycle and probable responses to climatic warming. Ecol. Appl. 1 (2), 182–195.

Hammond, J.C., Harpold, A.A., Weiss, S., Kampf, S.K., 2019. Partitioning snowmelt and rainfall in the critical zone: Effects of climate type and soil properties. Hydrol. Earth Syst. Sci. 23 (9), 3553–3570. http://dx.doi.org/10.5194/hess-23-3553-2019.

Heldmyer, A., Livneh, B., Molotch, N.P., Rajagopalan, B., 2021. Investigating the relationship between peak snow-water equivalent and snow timing indices in the Western United States and Alaska. Water Resour. Res. http://dx.doi.org/10.1029/2020WR029395.

Hodgkins, G.A., Dudley, R.W., 2006. Changes in the timing of winter-spring streamflows in eastern North America, 1913–2002. Geophys. Res. Lett. 33, 6402. http://dx.doi.org/10.1029/2005GL025593.

Jyrkama, M.I., Sykes, J.F., 2007. The impact of climate change on spatially varying groundwater recharge in the grand river watershed (Ontario). J. Hydrol. 338 (3–4), 237–250. http://dx.doi.org/10.1016/j.jhydrol.2007.02.036.

Kane, D.L., Stein, J., 1983. Water movement into seasonally frozen soils. Water Resour. Res. 19 (6), 1547–1557. http://dx.doi.org/10.1029/WR019i006p01547, https://agupubs-onlinelibrary-wiley-com.ezp3.lib.umn.edu/doi/full/10.1029/WR019i006p01547.

Leibowitz, S.G., Vining, K.C., 2003. Temporal connectivity in a prairie pothole complex. Wetlands 23 (1), 13–25.

Leuthold, S.J., Ewing, S.A., Payn, R.A., Miller, F.R., Custer, S.G., 2021. Seasonal connections between meteoric water and streamflow generation along a mountain headwater stream. Hydrol. Process. 35 (2), http://dx.doi.org/10.1002/hyp.14029, https://onlinelibrary.wiley.com/doi/10.1002/hyp.14029.

Lindström, G., Bishop, K., Löfvenius, M.O., 2002. Soil frost and runoff at Svartberget, Northern Sweden - Measurements and model analysis. Hydrol. Process. 16 (17), 3379–3392. http://dx.doi.org/10.1002/hyp.1106.

McDonnell, J.J., Spence, C., Karran, D.J., van Meerveld, H.J.I., Harman, C.J., 2021. Fill-and-spill: A process description of runoff generation at the scale of the beholder. Water Resour. Res. 57 (5), http://dx.doi.org/10.1029/2020WR027514, https://onlinelibrary.wiley.com/doi/10.1029/2020WR027514.

Mellander, P.-E., Stähli, M., Gustafsson, D., Bishop, K., 2006. Modelling the effect of low soil temperatures on transpiration by Scots pine. Hydrol. Process. 20 (9), 1929–1944. http://dx.doi.org/10.1002/hyp.6045, www.interscience.wiley.com https://onlinelibrary.wiley.com/doi/10.1002/hyp.6045.

Murray, K., Conner, M.M., 2009. Methods to quantify variable importance: Implications for the analysis of noisy ecological data. Ecology 90 (2), 348–355. http://dx.doi.org/10.1890/07-1929.1, http://doi.wiley.com/10.1890/07-1929.1.

Musselman, K.N., Addor, N., Vano, J.A., Molotch, N.P., 2021. Winter melt trends portend widespread declines in snow water resources. Nature Clim. Change http://dx.doi.org/10.1038/s41558-021-01014-9.

Pringle, C., 2003. What is hydrologic connectivity and why is it ecologically important? Hydrol. Process. Invit. Comment. 17, 2685–2689. http://dx.doi.org/10.1002/hyp.5145, www.interscience.wiley.com.

Richardson, M.C., Mitchell, C.P.J., Branfireun, B.A., Kolka, R.K., 2010. Analysis of airborne LiDAR surveys to quantify the characteristic morphologies of northern forested wetlands. J. Geophys. Res. Biogeosci. 115 (3), http://dx.doi.org/10.1029/2009JG000972.

Ryberg, K.R., Akyüz, F.A., Wiche, G.J., Lin, W., 2016. Changes in seasonality and timing of peak streamflow in snow and semi-arid climates of the north-central United States, 1910–2012. Hydrol. Process. 30 (8), 1208–1218. http://dx.doi.org/10.1002/hyp.10693, http://nwis.waterdata.usgs.gov/usa/ https://onlinelibrary.wiley.com/doi/10.1002/hyp.10693.

Schneider, D., Molotch, N.P., 2016. Real-time estimation of snow water equivalent in the upper Colorado river basin using MODIS-based SWE reconstructions and SNOTEL data. Water Resour. Res. 52 (10), 7892–7910. http://dx.doi.org/10.1002/2016WR019067, http://www.wcc.nrcs.usda.gov/snow/.

Sebestyen, S., Burdick, J.M., Roman, D.T., Lany, N.K., Kyllander, R.L., Elling, A., Verry, E.S., Kolka, R.K., 2021a. Marcell Experimental Forest Daily Peatland Water Table Elevation, 1961 - Ongoing, second ed. USDA Forest Service, Environmental Data Initiative, http://dx.doi.org/10.6073/pasta/2a75c323256252a763e9343f0df7b6af.

Sebestyen, S., Dorrance, C., Olson, D., Verry, E., Kolka, R., Elling, A., Kyllander, R., 2011. Long-term monitoring sites and trends at the marcell experimental forest. In: Peatland Biogeochemistry and Watershed Hydrology at the Marcell Experimental Forest. CRC Press, pp. 15–71. http://dx.doi.org/10.1201/b10708-3, http://www.crcnetbase.com/doi/10.1201/b10708-3.

Sebestyen, S., Lany, N.K., Roman, D.T., Burdick, J.M., Kyllander, R.L., Verry, E.S., Kolka, R.K., 2021b. Hydrological and meteorological data from research catchments at the Marcell Experimental Forest, Minnesota, USA. Hydrol. Process. 35 (3), http://dx.doi.org/10.1002/hyp.14092.

Shanley, J.B., Chalmers, A., 1999. The effect of frozen soil on snowmelt runoff at Sleepers River, Vermont. Hydrol. Process. 13, 1843–1857.

Trujillo, E., Molotch, N.P., 2014. Snowpack regimes of the Western United States. Water Resour. Res. (50), 5375–5377. http://dx.doi.org/10.1002/2013WR014979.Reply.

Verry, E.S., Brooks, K.N., Nichols, D.S., Ferris, D.R., Sebestyen, S.D., 2011. Watershed hydrology. In: Peatland Biogeochemistry and Watershed Hydrology at the Marcell Experimental Forest. CRC Press, pp. 193–212. http://dx.doi.org/10.1201/b10708-8.

Verry, E.S., Elling, A., Sebestyen, S., Kolka, R.K., Kyllander, R.L., 2018. Marcell Experimental Forest Daily Streamflow Data, 1 Ed. Forest Service Research Data Archive, Fort Collins, Co., http://dx.doi.org/10.2737/RDS-2018-0009.

Virtanen, P., Gommers, R., Oliphant, T.E., Haberland, M., Reddy, T., Cournapeau, D., Burovski, E., Peterson, P., Weckesser, W., Bright, J., van der Walt, S.J., Brett, M., Wilson, J., Millman, K.J., Mayorov, N., Nelson, A.R.J., Jones, E., Kern, R., Larson, E., Carey, C.J., Polat, I., Feng, Y., Moore, E.W., VanderPlas, J., Laxalde, D., Perktold, J., Cimrman, R., Henriksen, I., Quintero, E.A., Harris, C.R., Archibald, A.M., Ribeiro, A.H., Pedregosa, F., van Mulbregt, P., Contributors, S., 2020. SciPy 1.0: Fundamental algorithms for scientific computing in Python. Nature Methods 17, 261–272. http://dx.doi.org/10.1038/s41592-019-0686-2, https://rdcu.be/b08Wh.

Winter, T.C., LaBaugh, J.W., 2003. Hydrologic considerations in defining isolated wetlands. Wetlands 23 (3), 532–540. http://dx.doi.org/10.1672/0277-5212(2003)023[0532:HCIDIW]2.0.CO;2.

Zhao, L., Gray, D.M., 1999. Estimating snowmelt infltration into frozen soils. Hydrol. Process. 13, 1827–1842.